Magnetic and transport properties of transparent $SrSn_{0.9}Sb_{0.05}Fe_{0.05}O_3$ semiconductor films

G. Prathiba, S. Venkatesh, K. Kamala Bharathi, and N. Harish Kumar'

Citation: J. Appl. Phys. **109**, 07C320 (2011); doi: 10.1063/1.3556693
View online: http://dx.doi.org/10.1063/1.3556693
View Table of Contents: http://aip.scitation.org/toc/jap/109/7
Published by the American Institute of Physics

Magnetic and transport properties of transparent $SrSn_{0.9}Sb_{0.05}Fe_{0.05}O_3$ semiconductor films

G. Prathiba,[1] S. Venkatesh,[2] K. Kamala Bharathi,[3] and N. Harish Kumar[1,a)]
[1]*Advanced Magnetic Materials Laboratory, Department of Physics, Indian Institute of Technology Madras, Chennai 600036, India*
[2]*Department of Condensed Matter Physics and Material Sciences, Tata Institute of Fundamental Research, Homi Bhabha Road, Mumbai 400 005, India*
[3]*Department of Mechanical Engineering, University of Texas at El Paso, El Paso, Texas 79968, USA*

(Presented 17 November 2010; received 24 September 2010; accepted 18 November 2010; published online 4 April 2011)

The effect of antimony doping on the structural, magnetic, and electrical properties of transparent $SrSn_{0.9}Sb_{0.05}Fe_{0.05}O_3$ films synthesized by RF sputtering on oxidized Si and quartz substrates has been investigated. A reduction in electrical resistivity by two orders of magnitude compared to 5% Fe doped $SrSnO_3$ film was observed. The electrical conductivity behavior has been analyzed using the Mott's Variable range hopping model. The nature of magnetic ordering were investigated by field cooled (FC) and zero field cooled (ZFC) magnetization measurements. The applicability of models based on oxygen vacancies to explain the magnetic ordering present in the sample has been discussed. © *2011 American Institute of Physics*. [doi:10.1063/1.3556693]

The efficiency of novel multifunctional devices that require fabrication of heterostructures depends upon the quality of interface.[1] Hence, they can be built by depositing thin layers of isostructural materials with different desirable properties. Perovskite oxides with interesting properties such as superconductivity, ferroelectricity, magnetism, multiferroicity, half metallicity, etc., within one structural family can be used for building such heterostructures.[2–4] Using them the charge,[5] spin,[6] and orbital[7] degrees of freedom can be controlled and manipulated at the interfaces.

Transparent magnetic semiconductors are attractive materials for multifunctional magneto-opto-electronic devices. Following the prediction of Dietl et al.,[8] on possible ferromagnetic ordering in wide bandgap semiconductors doped with magnetic elements, the focus was on oxide dilute magnetic semiconductors (O-DMS).[9]

Perovskite alkaline earth stannates have interesting dielectric and gas sensing properties.[10,11] Employing them, single flux quantum circuits were built using all perovskite hetero structures.[12,13] $SrSnO_3$ is a wide bandgap perovskite oxide with a direct bandgap of 4.27 eV. At room temperature it crystallizes in orthorhombic perovskite structure.[14] For spin based multifunctional devices using O-DMS it is vital to develop materials in which defect concentration can control the electrical and magnetic properties. In our earlier work room temperature ferromagnetism was observed in bulk polycrystalline Fe doped $SrSnO_3$.[15] The electronic structure calculations showed them to be half metallic. All the compositions show semiconducting behavior. The conductivity increases with Fe concentration, as the activation energy decreases. Optical transparency makes the films a feasible candidate for magneto-opto-electronic applications.

Sb doped $SrSnO_3$ films are conducting and transparent.[16] In this work a co-doping of 5% Sb and Fe to $SrSnO_3$ [$SrSn_{0.9}Sb_{0.05}Fe_{0.05}O_3$] was tried to decrease the resistivity without affecting the transparent nature. The defect concentration was found to control the electrical and magnetic properties effectively.

Polycrystalline $SrSn_{0.9}Sb_{0.05}Fe_{0.05}O_3$ synthesized by solid state reaction with high pure chemicals (Alfa Aeser 99.99%) was made into 2 in. diameter targets. The films were deposited on oxidized silicon (100) and quartz substrates by radio frequency (RF) magnetron sputtering. The chamber was evacuated to a base pressure of 5×10^{-6} Torr and the sputtering carried out using Ar gas at 1.7×10^{-2} Torr pressure. During deposition oxygen was not introduced into the chamber. The films were deposited on ultrasonically cleaned substrates maintained at room temperature. The films were post annealed at 1073 K for 2 h in air.

Structural characterization was performed using X-ray Diffraction (XRD) technique employing CuK_α radiation. The surface morphology was studied by a Scanning Probe Microscope (SPM). Magnetization measurements were carried out employing a SQUID magnetometer up to 2 T, with the magnetic field applied parallel to the plane of the film from room temperature to 1.8 K. The zero field cooled (ZFC) and field cooled (FC) magnetization was measured at 100 Oe. The optical transmittance spectra was obtained using a CARY 5E UV–Vis spectrophotometer. The resistivity of the film was measured from 100 K to RT by a two probe method using a Keithley electrometer and a closed cycle refrigerator (CCR).

The XRD shows that the as-deposited films are amorphous but turn polycrystalline (Fig. 1) upon annealing. At room temperature $SrSnO_3$ crystallizes in orthorhombically distorted perovskite structure in the space group Pbnm with lattice parameters $a = 5.707$ Å, $b = 5.707$ Å and $c = 8.064$ Å.[14] The thickness of the film was found to be around 100 nm.

a)Author to whom correspondence should be addressed; Electronic mail: harish@physics.iitm.ac.in.

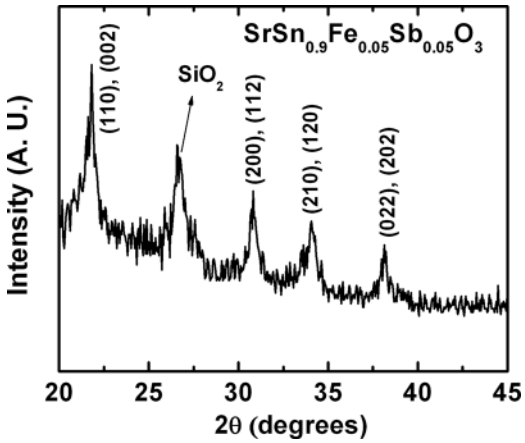

FIG. 1. X-ray scan for $SrSn_{0.9}Sb_{0.05}Fe_{0.05}O_3$ film grown on oxidized Si (100) substrate.

The crystallite size and the strain factor were estimated from the XRD data using the Scherrer[17] calculator in Panalytical's X'pert High Score Plus software which uses the Pseudo-Voigt profile function for the analysis. The average crystallite size and strain factor were found to be around 40 nm and 0.7% respectively.

The analysis of XRD data of films shows them to be single phase. The scanning electron microscope (SEM) investigations could not be carried out on the films due to the low thickness (100 nm) of the films. However a backscattered electron (BSE) image taken using SEM on the target did not show any trace of secondary phase. Hence, we presume that the phase purity of the films is at least 95% which is the limit of resolution for XRD measurement.

The high resolution AFM image of the film shows (Fig. 2) fine microstructure and uniform distribution of dense particles spherical in shape. The room mean square value of surface roughness is 6.88 nm. The average particle size is 45 nm which is close to the crystallite size estimated from the XRD data.

The magnetization measured as a function of magnetic field (M vs H) at 300 K and 1.8 K is shown in Fig. 3 after

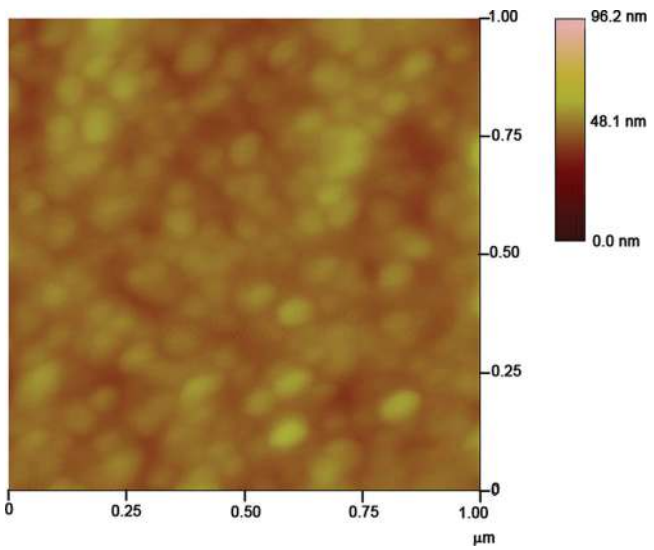

FIG. 2. (Color online) SPM image of $SrSn_{0.9}Sb_{0.05}Fe_{0.05}O_3$ film.

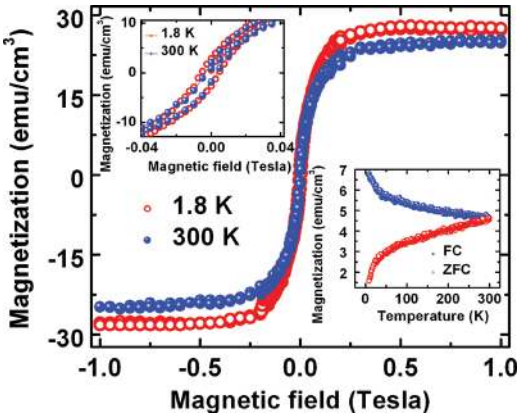

FIG. 3. (Color online) Isothermal field variation of magnetization for $SrSn_{0.9}Sb_{0.05}Fe_{0.05}O_3$ film at 1.8 K (open circle) and 300 K (closed circle). Inset 1 shows the enlarged image of the field variation of magnetization showing a hysteresis loop, Inset 2 shows the ZFC (open circle) and FC (closed circle) magnetization curves at 100 Oe from 1.8 to 300 K.

subtracting the diamagnetic contribution from the substrate. A hysteresis loop with a coercive field (H_c) of 60 Oe and 95 Oe (Inset 1) was observed at 300 K and 1.8 K respectively. Inset 2 of Fig. 3 shows the zero field cooled (ZFC) and the field cooled (FC) magnetization curves recorded at 100 Oe. The magnetic hysteresis at RT and the absence of any magnetic transition in the temperature range 1.8 to 300 K indicate that the Curie temperature is above RT.

The optical transmission spectra for the wavelength range 200–1000 nm (Fig. 4) exhibit high transparency (above 80%) except where the incident radiation is absorbed across the bandgap (E_g). The inset shows the plot of $(\alpha h\nu)^2$ vs photon energy ($h\nu$) where α is the absorption coefficient. $SrSn_{0.9}Sb_{0.05}Fe_{0.05}O_3$ was found to be a direct bandgap material with a bandgap of 4.6 eV. The small increase in the bandgap value for the thin film when compared to the bulk is most likely attributed to the quantum confinement effect due to the presence of nanocrystalline grains.[18]

The electrical conductivity of the $SrSn_{0.9}Sb_{0.05}Fe_{0.05}O_3$ film decreases exponentially with decrease in temperature indicating their semiconducting nature (Fig. 5). The room temperature resistivity (4.184 Ω) is 2 orders less than that of

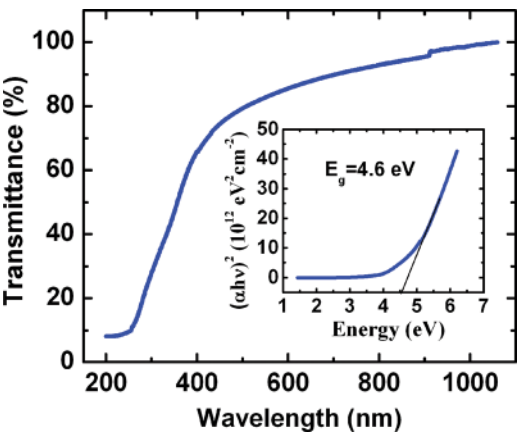

FIG. 4. (Color online) Optical transmission spectra of $SrSn_{0.9}Sb_{0.05}Fe_{0.05}O_3$ film grown on quartz substrate. The inset shows the plot between $(\alpha h\nu)^2$ and photon energy ($h\nu$).

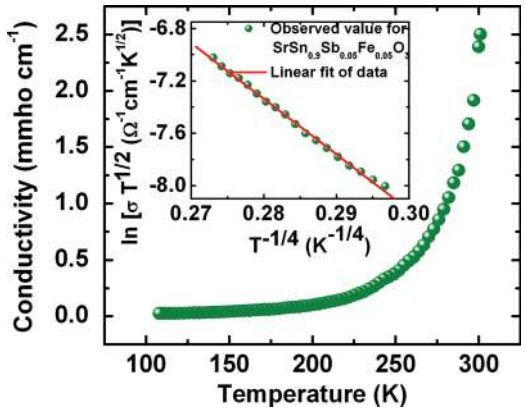

FIG. 5. (Color online) Conductivity as a function of temperature. Inset shows the linear fit of $\ln(\sigma T^{[1/2]})$ vs $T^{-1/4}$ for $SrSn_{0.9}Sb_{0.05}Fe_{0.05}O_3$ film.

5% Fe doped $SrSnO_3$ films (229 Ω).[19] The decrease in resistivity can be explained by the production of random potential on antimony doping, which in turn has led to the formation of large number of localized states.[16]

Mott's variable range hopping (VRH) model[20,21] was used to explain the conduction mechanism present in the sample, which is given by $\sigma T^{1/2} = A \exp(-BT^{-1/4})$ where *A* and *B* are constants and *B* is expressed as $B = 2.1[\alpha^3/K_B N(E_F)]^{1/4}$ where $N(E_F)$ is the density of localized states at E_F and α^{-1} is the decay constant of the wave function of localized states at E_F. A good fit to the experimental data (inset of Fig. 5) gives A = 4.55, B = 42.45 K and VRH radius $r_{VRH} = 1/\alpha = 2.32$ nm.

The nature of magnetic ordering in O-DMS has been a subject of intense debate. The possible origin for the magnetic response of the films has been investigated by isothermal magnetization measurements as well as ZFC and FC measurements. The ZFC curve did not show any cusp or a peak characteristic of superparamagnetic systems. Further the ZFC and FC magnetization curves measured at a field of 100 Oe is well separated up to room temperature, which rules out the possibility of superparamagnetism below RT. Similar behavior has been observed in ferromagnetic $TiO_{2-\delta}$ nano particles and ZnO powders.[22,23] The analysis of XRD, magnetic response and electrical transport characteristics did not indicate any effect of secondary phase.

To get oxygen deficient $SrSn_{0.9}Sb_{0.05}Fe_{0.05}O_3$ films, they were deposited in 100% Ar atmosphere and annealed in air. Since the chance of oxygen deficiency is more in these films and also the other possible origins of magnetic ordering were ruled out Coey's donor impurity band exchange mechanism[24] and concentric bounded model[25] was used to explain the magnetic response.

The bound magnetic polaron (BMP) radius according to Coey's model, calculated from the formula $R_{BMP} = \epsilon(m/m^*)a_o$, was found to be around 0.49 nm. According to the concentric bounded model a larger VRH sphere around the smaller BMP sphere explains the long range ordering and electric conduction properties in the Dilute Magnetic Oxides, which evolves as a function of defect concentration.

The localized carriers couples strongly with the neighboring impurity ions (doped magnetic iron), thus forming the bound magnetic polaron in the inner sphere and can itinerate with no spin coherence in the outer shell. Using the Mott's variable–range hopping model in fitting the resistivity to temperature curves showed that the localized radii ($r_{VRH} = 2.32$ nm) of the localized carriers are larger than that of the BMP model ($r_{BMP} = 0.49$ nm). Carriers move either by spin-polarized or spin independent variable–range hopping between concentric spheres.

In summary, $SrSn_{0.9}Sb_{0.05}Fe_{0.05}O_3$ films were fabricated on oxidized Si (100) and quartz substrates by RF sputtering method. The annealed films were polycrystalline with the average crystallite size 40 nm. The film is optically transparent, having transmittance above 80% in the visible region with bandgap 4.6 eV. The electrical conductivity in this material follows the Mott's Variable range hopping model. The resistivity of $SrSn_{0.9}Sb_{0.05}Fe_{0.05}O_3$ film [$\rho_{RT} = 4.184$ Ωm] is 2 orders of magnitude less than $SrSn_{0.95}Fe_{0.05}O_3$ films [$\rho_{RT} = 229$ Ωm]. The magnetic response of the films does not seem to indicate superparamagnetism. Hence the oxygen vacancy based models were used to qualitatively explain the observed magnetic and transport properties.

The authors N.H.K. and G.P. thank NRB, India for their financial support. G.P. also thanks IIT, Madras for their financial support.

[1]J. Heber, Nature (London) **459**, 28 (2009).
[2]M. W. J. Prins *et al.*, Appl. Phys. Lett. **68**, 3650 (1996).
[3]J. Siddiqui *et al.*, Appl. Phys. Lett. **88**, 212903 (2006).
[4]K. Shibuya *et al.*, Appl. Phys. Lett. **85**, 425 (2004).
[5]A. Ohtomo and H. Y. Hwang, Nature (London) **427**, 423 (2004).
[6]K. Ueda, H. Tabata, and T. Kawai, Science **280**, 1064 (1998).
[7]J. Chakhalian *et al.*, Science **318**, 1114 (2007).
[8]T. Dietl *et al.*, Science **287**, 1018 (2000).
[9]W. Prellier *et al.*, J. Phys. Condens. Matter. **15**, R1583 (2003).
[10]L. Geske *et al.*, J. Eur. Ceram. Soc. **25**, 2537 (2005).
[11]E. H. Mountstevens *et al.*, J. Phys. Condens. Matter. **15**, 8315 (2003).
[12]H. Wakana *et al.*, IEEE Trans. Appl. Supercond. **15**, 153 (2005).
[13]K. Chiba *et al.*, IEEE Trans. Appl. Supercond. **11**, 2734 (2001).
[14]A. Vegas *et al.*, Acta. Crystallogr. B. **42**, 167 (1986).
[15]G. Prathiba *et al.*, Solid. State. Comm. **150**, 1436 (2010).
[16]Q. Z. Liu *et al.*, J. Appl. Phys. **103**, 093709 (2008).
[17]B. D. Cullity and S. R. Stock, *Elements of X-ray Diffraction* (Prentice Hall, 2001).
[18]S. K. Gullapalli *et al.*, Appl. Phy. Lett. **96**, 171903 (2010).
[19]G. Prathiba *et al.* (Communication).
[20]N. F. Mott and E. A. Davis, *Electronic Processes in Non-Crystalline Materials*, 2nd Ed. (Clarendon, Oxford, 1979).
[21]M. G. Hutchins *et al.*, J. Phys. Condens. Matter. **18**, 9987 (2006).
[22]Q. Zhao *et al.*, J. Appl. Phys. **104**, 073911 (2008).
[23]S. Banerjee *et al.*, Appl. Phys. Lett. **91**, 182501 (2007).
[24]J. M. D. Coey *et al.*, Nat. Mater. **4**, 173 (2005).
[25]H. Chou *et al.*, Phys. Rev. B. **77**, 245210 (2008).